Jurnal
Teknologi

Full Paper

UPTAKE BEHAVIOR OF ARSENATE FROM AQUEOUS SOLUTION USING FERRIC-COATED MESOPOROUS CERAMIC ADSORBENT

Borano Te, Boonchai Wichitsathian*, Chatpet Yossapol

School Of Environmental Engineering, Institute Of Engineering, Suranaree University Of Technology, Nakhon Ratchasima 30000, Thailand

*Corresponding author
boonchai@sut.ac.th

Article history
Received
25 June 2015
Received in revised form
21 September 2015
Accepted
23 December 2015

Graphical abstract

Abstract

Broken mesoporous ceramic filter was reutilized by coating with ferric solution through a simple loading method enhanced with heating at a moderate temperature for arsenate uptake from aqueous solution. BET, XRF, XRD, and SEM methods were applied for the adsorbent characterization. The adsorption study was conducted in a batch mode to investigate kinetics, isotherms, and the effect of solution pH and co-existing anions. The pseudo-second order kinetic model well fitted the experimental data (R^2 = 0.9997). The maximum arsenate adsorption capacity (2.27 mg/g) was derived from the better described Langmuir isotherm model (R^2 = 0.9992). The adsorbent expressed high arsenate adsorption capacity over a pH range of 4-10. The uptake behavior is a favorable and physical adsorption process based on the value of separation factor and mean sorption energy. The presence of co-existing anions decreased the arsenate adsorption capacity in the following order: NO_3^-< SO_4^{2-} < PO_4^{3-}. The new ferric-coated mesoporous ceramic adsorbent could be an effective and low-cost adsorbent for arsenate removal from water.

Keywords: Adsorption, mesoporous adsorbent, kinetics, isotherms, co-existing anions

1.0 INTRODUCTION

Arsenic is one of the most highly toxic and carcinogenic elements. Excessive and long-term exposure to arsenic contaminated media possibly results in several health hazards such as skin, kidney, bladder, and lung cancers as well as diabetes, cardiovascular disease, adverse pregnancy outcomes, and neurological problem [1, 2]. The World Health Organization introduces a new maximum contaminant level of arsenic in drinking water to 10 ppb from 50 ppb [3]. The issue of arsenic contamination on water sources is a global phenomenon. More than 70 countries are reported with concentrated arsenic contamination posing a health risk to an estimated 150 million people, most of which live in countries such as Bangladesh, Cambodia, China, India, Laos, Myanmar, Nepal, Pakistan, Taiwan and Vietnam [4].

The major arsenic forms in natural water are arsenate and arsenite. Arsenite predominates in reducing environments like groundwater, whereas arsenate predominates in oxygen-rich environments like surface water [5]. Arsenite is generally oxidized to arsenate before being removed from water. Technically, arsenate in water cannot be easily remediated or removed through simple practices like boiling or leaving to open air. Several technologies reported to remove arsenic from water include precipitation, ion exchange, membrane technologies, reverse osmosis and adsorption processes. Adsorption process, a widely used method to remove pollutants from water, has more advantages in terms of simplicity, economy, removal efficiency, easiness in operation and maintenance, flexibility to be scaled up, and avoidance of liquid waste generation on site [6]. Many materials that have been used as sorbents include commercial and synthetic activated carbons,

agricultural product or by-products, industrial by-products or wastes, and metal oxides [7]. Typically, the adsorption capacity of natural adsorbents is lower than that of synthetic or modified adsorbents. Among several modification techniques, iron coating or impregnation seems to be simple, cost-effective, and removal efficiency-improved and gains more popularity to be applied for developing an efficient adsorbent for pollutant removal [8-11].

The study aims to reutilize ceramic water filters, primarily being a filter to provide drinking water free from bacteria and turbidity but broken in the production and piled up as a solid waste without further use, as a raw material to be modified with ferric solution to be a more efficient and low-cost adsorbent for arsenate removal from aqueous solution.

2.0 MATERIALS AND METHODS

All experiments were conducted with analytical grade reagents without any further purification. Arsenate stock solutions (100 mg/L) were prepared by dissolving appropriate amount of sodium hydrogen arsenate ($Na_2HAsO_4 \cdot 7H_2O$, Sigma-Aldrich) in ultrapure water. Ferric solution was obtained from $FeCl_3 \cdot 6H_2O$. $NaNO_3$, Na_2SO_4, and KH_2PO_4 were used to produce co-existing anions including nitrate (NO_3^-), sulfate (SO_4^{2-}), and phosphate (PO_4^{3-}), respectively. The solution pH was adjusted with 0.1M HCl and/or NaOH.

The porous ceramic filter is made by mixing clay, fine ground rice husk and water. The mixture is then molded and heated at approximately 800˚C for about 3 h for water filtration. The samples were collected from the pile of broken filter at a local factory, washed several times with tap water, and dried under hot sun. The dried samples were ground and sieved to obtain particle size of 0.6-1.18mm. The particles were washed several times with deionized (DI) water and dried in a hot air flow oven at 60˚C for 24 h. Upon cooling, the particles were kept in a dry and clean container and labeled as PC. To modify with ferric solution, 100g of PC was soaked with 100 mL of 2.5M $FeCl_3 \cdot 6H_2O$. The mixture was thoroughly mixed, dried at 60˚C for 3 h, and further heated at a moderate temperature (400˚C) for about 2 h to ensure higher effective affinity of iron on the surface. After being cooled to room temperature, the materials were washed with DI water until no reddish color. Finally, it was dried at 60˚C for 24 h in a hot air flow oven and labeled as PC/$FeCl_3$ for using in the further experiments.

The chemical composition analysis of PC and PC/$FeCl_3$ was carried out with Energy Dispersive X-ray Fluorescence. The XRD investigation for mineralogical phases was performed using the Bruker XRD (D2 PHASER). Surface area, pore volume, and average pore diameter were obtained by Brunauer-Emmett-Teller (BET) methods using the BET analyzer (BELSORP Mini II, BEL Inc., Japan). The morphological features of PC and PC/$FeCl_3$ were examined by a scanning electron microscope (SEM, JSM-6010LV, JEOL, Japan).

The adsorption experiments were conducted in a batch mode. Kinetic experiments were carried out at temperature (27±1˚C) in the 500 mL Erlenmeyer flasks with an agitation speed of 150 rpm on a horizontal mechanical shaker. 400 mL of arsenate solution (10mg/L, pH=7±0.1) was adsorbed by 10 g/L of PC/$FeCl_3$. While the adsorption was taking place, samples were taken at preset time intervals. Isotherm study was carried out with arsenate concentrations from 0.5 to 40mg/L. The 250 ml flasks were filled with 50 mL of arsenate solution (pH=7±0.1) and 10 g/L of the adsorbent. The mixture was shaken with 150 rpm at temperature (27±1˚C) for an equilibrium time. The effect of pH was carried out in a pH range of 4 to 11 using 50 mL of arsenate solution (10mg/L) and 10g/L of the adsorbent. The effect of co-existing anions was investigated by adding 10 and 100mg/L of anions (NO_3^-, SO_4^{2-}, and PO_4^{3-}) to 10mg/L of arsenate solution. All the samples were filtered through a 0.22 µm syringe filter and kept at 4˚C until the time for arsenate analysis. The measurement of arsenate concentration was conducted by inductively coupled plasma-optical emission spectrometry (ICP-OES) (Optima 8000, PerkinElmer, USA) using a wavelength of 193.7 nm. The amount of arsenate adsorbed per unit mass of the adsorbent, q_e(mg/g), was determined by the following equation:

$$q_e = \frac{(C_o - C_e)}{M} \times V \quad (1)$$

where C_o and C_e (mg/L) are the initial and equilibrium arsenate concentration, respectively; V (L) is the used volume of the solution; and M (g) is the mass of the adsorbent.

3.0 RESULTS AND DISCUSSION

3.1 Characterization of Adsorbent

The properties of PC and PC/$FeCl_3$ are shown in Table 1. The results indicated that the surface area and pore volume were increased after ferric coating, whereas the average pore diameter was decreased probably due to the attachment of iron ion on the surface of the raw material. Furthermore, the average pore sizes of PC and PC/$FeCl_3$ were within 2-50 nm, indicating that the materials are mesoporous according to the pore classification recommendation of the International Union of Pure and Applied Chemistry [12]. Chemical composition analysis showed that silica, alumina and iron oxide were the major constituents of both PC and PC/$FeCl_3$. After being treated with ferric solution, the percentage of silica and alumina decreased from 71.23% to 66.73% and 21.44% to 20.59%, respectively, whereas the percentage of iron oxide increased from 4.17% to 9.17%.

Table 1 Chemical composition (%w/w) and physical properties of PC and $PC/FeCl_3$

Adsorbents	SiO_2	Al_2O_3	Fe_2O_3	K_2O	TiO_2	CaO	MnO_2	Surface area (m^2/g)	Pore volume (cm^3/g)	Average pore diameter (nm)
PC	71.23	21.44	4.17	1.86	0.90	0.26	0.10	5.08	0.04	31.04
$PC/FeCl_3$	66.73	20.59	9.17	1.84	0.69	0.22	0.06	7.09	0.05	25.91

This implied that some proportions of silicon and alumina of PC were corroded due to the acid condition of ferric solution and the ferric coating increased the iron proportion. Figure 1 represents the surface morphological features of PC and $PC/FeCl_3$, respectively. PC forms a rough surface structure and $PC/FeCl_3$ appears to have a smother surface having some pores filling up with flocculent particles shape. The XRD patterns of PC and $PC/FeCl_3$ are illustrated in Figure 2. The patterns were identical for most of the parts, however, the occurrences of several new peaks and the increase in the intensity of the peaks were observed for the patterns of $PC/FeCl_3$. This may be due to the increase in the amount of iron oxide on the surface. The major mineral constituents of both PC and $PC/FeCl_3$ include quartz, montmorillonite, and hematite.

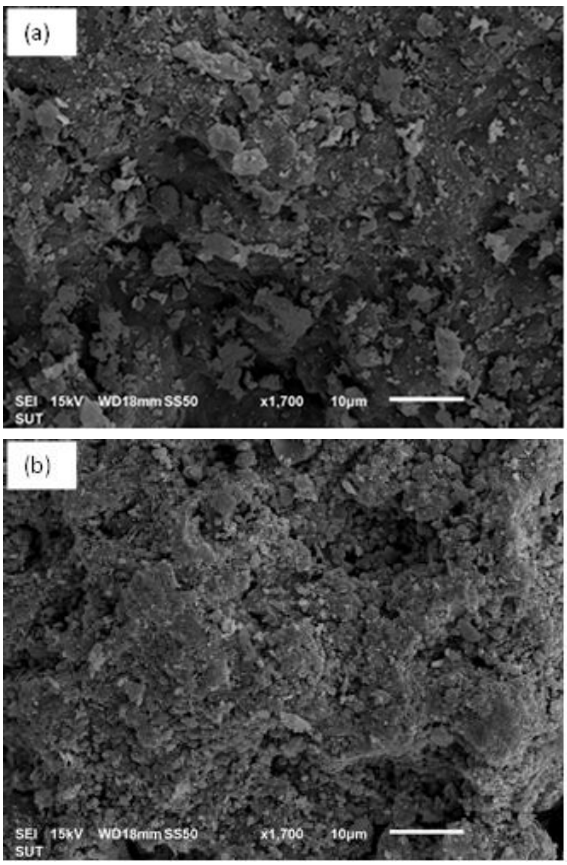

Figure 1 SEM images of (a) raw material (PC) and (b) ferric-coated adsorbent ($PC/FeCl_3$)

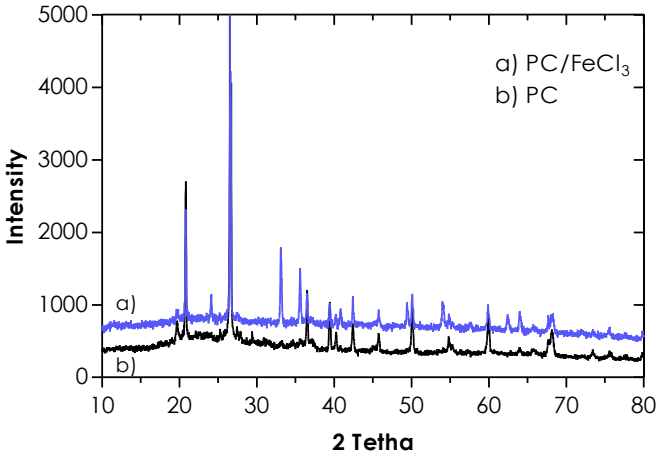

Figure 2 X-ray diffraction pattern of PC and $PC/FeCl_3$

3.2 Contact Time and Kinetic Study

The contact time was observed over a period of 32 h. The adsorption capacity at certain time and the kinetic models used to predict the experimental kinetic data are presented in Figure 3. It clearly indicates that the adsorption occurred fast within the first 5h, reaching adsorption capacity of 0.822 mg/g accounting for more than 80% of the maximum adsorption capacity. The adsorption speed gradually slowed down and stabilized afterwards within 24 h.

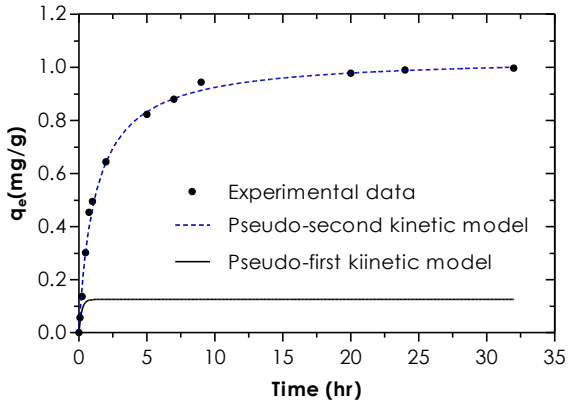

Figure 3 Kinetics of arsenate adsorption onto $PC/FeCl_3$ with the experimental conditions (arsenate: 10mg/L, dosage: 10g/L, temperature: 27±1˚C, rpm= 150, pH=7±0.1)

This may be explained by the reason that the adsorbent initially possesses more active sites on its surface and is later filled up till reaching its equilibrium [13]. To predict the kinetic experimental data, the pseudo-first order and pseudo-second order models with linearized equations shown in equation (2) and (3), respectively, were applied.

$$\ln(q_e - q_t) = \ln q_e - k_1 t \quad (2)$$

$$\frac{t}{q_t} = \frac{1}{k_2 q_e^2} + \frac{t}{q_e} \quad (3)$$

where q_t (mg/g) is the amount of arsenate adsorbed at time t; q_e (mg/g) is the amount of arsenate adsorbed at equilibrium time; k_1 (1/h) is the rate constant of the pseudo-first order model; k_2 (g/mg/h) is the rate constant of the pseudo-second order model.

The kinetic parameters including kinetic constants, calculated equilibrium adsorption capacity and correlation coefficient are presented in Table 2. The value of correlation coefficient (R^2) and the comparison between the adsorption capacity from experiment and calculation were used to determine which kinetic model was a better fitting model to the experimental kinetic data. The results showed that the correlation coefficient value of the pseudo-second order model (R^2 = 0.9997) was higher than that of the pseudo-first order model (R^2 = 0.9542). The adsorption capacity of experiment and calculation in the pseudo-second order are close enough. Therefore, it is concluded that the adsorption kinetics can be better described with the pseudo-second order rate model. This implied that the amount of arsenate adsorbed at equilibrium possibly represents the binding sites of the adsorbent [14].

3.3 Effect of pH

The adsorption capacity of arsenate by PC/$FeCl_3$ over the studied range of solution pH is illustrated in Figure 4. The result showed that the adsorbent possesses a high arsenate adsorption capacity over a wide pH range. Arsenate uptake capacity from 0.956 to 0.983mg/g was observed for the value of pH from 4 to 10. Then, the adsorption capacity dramatically decreased to around 0.242mg/g when pH was increased from 10 to 11. The high arsenate adsorption capacity over a wide pH range can be explained by the reasons that arsenate largely occurs in less negative charge species for pH from 2.2 to 11.5, and the adsorbent has the capacity to buffer the solution pH. Arsenate species in aqueous phase exist mainly as H_3AsO_4 at pH less than 2.2, $H_2AsO_4^-$ at pH between 2.2 and 6.98, $HAsO_4^{2-}$ at pH between 6.98 and 11.5, and AsO_4^{3-} at pH above 11.5 [15]. The one or two negative charge of arsenate species may require less electrostatic attraction force to attach on the positive charge of ferric species on the adsorbent. The possession of the pH buffering capacity of the adsorbent is possibly due to the presence of the high content of amphoteric-in-nature Fe oxide [16]. The significant decrease in the arsenate adsorption for pH more than 11 may be due to the increase in the negative charge site on the surface of the adsorbent [17].

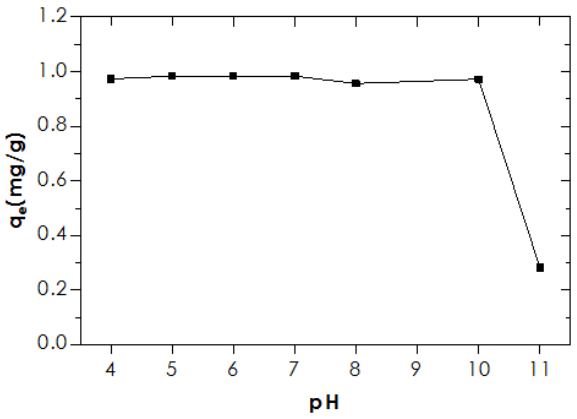

Figure 4 Effect of pH on arsenate adsorption by PC/$FeCl_3$ with the experimental conditions (arsenate: 10mg/L, dosage: 10g/L, temperature: 27±1°C, rpm: 150, contact time=24h)

3.4 Isotherm Study

The relationship between the adsorption capacity (mg/g) and the equilibrium concentration (mg/L) within the equilibrium time allows the adsorption isotherm to be understood, and possibly be used to determine the characteristics of the adsorption and maximum adsorption capacity of the adsorbent. Isotherm models including the Langmuir, the Freundlich and the Dubinin-Radushkevich (D-R) were used to predict the equilibrium isotherm data in this study. The linearized equation forms of the Freundlich and Langmuir isotherm models are expressed in equation (4) and (5), respectively:

$$\ln q_e = \ln K_F + (1/n) \ln C_e \quad (4)$$

Table 2 Kinetic parameters of arsenate adsorption onto $PC/FeCl_3$

Adsorbents	q_e(exp.)(mg/g)	Pseudo-first order model			Pseudo-second order model		
		q_e(cal.)(mg/g)	k_1(1/h)	R^2	q_e(cal.)(mg/g)	k_2(g/mg/h)	R^2
$PC/FeCl_3$	0.996	0.125	4.929	0.9542	1.039	0.772	0.9997

$$\frac{C_e}{q_e} = \frac{1}{K_L q_{max}} + \frac{C_e}{q_{max}} \quad (5)$$

where C_e (mg/L) is the arsenate concentration at equilibrium; q_e (mg/g) is the amount of arsenate adsorbed at equilibrium per unit mass of the adsorbent; q_{max} (mg/g) is the maximum adsorption capacity based on the Langmuir equation; K_L (L/mg) is the Langmuir constant; K_F ($mg^{1-1/n}L^{1/n}/g$) is the adsorption coefficient from the Freundlich equation. The values of K_L and q_{max} were calculated from the intercept and slope of the linear plot of (C_e/q_e) against C_e, respectively. The values of 1/n and K_F were determined from the slope and intercept of the plot of $\ln q_e$ versus $\ln C_e$, respectively.

The experimental isotherm data and the fitting isotherm model are illustrated in Figure 5. The values of the maximum adsorption capacity, isotherm constants, and correlation coefficient of the models are given in Table 3. The correlation coefficient (R^2) of the Langmuir and Freundlich were 0.9992 and 0.8703, respectively, indicating the experimental data fitted very well to the Langmuir model. This implies that the arsenate adsorption occurs as the monolayer adsorption on the active surface site of the adsorbent. The maximum adsorption capacity of arsenate removal by the adsorbent was 2.27 mg/g. The characteristics of the adsorption can be determined through the value of a dimensionless constant separation factor (R_L). The separation factor was calculated by $R_L = 1/(1+K_L C_o)$, where C_o (mg/L) is the initial arsenate concentration. The adsorption process is irreversible (R_L=0), favorable (0<R_L<1), linear (R_L=1) and unfavorable (R_L>1) [18]. The values of R_L computed for this study were from 0.01 to 0.34 (within a range of 0-1). This implies that the uptake behavior of arsenate is a favorable adsorption.

The D-R model is used to evaluate the nature of adsorption as either physical or chemical favor through the estimation of mean sorption energy [20]. The linearized form of the model and the mean sorption energy are shown in equation (6) and (7), respectively.

$$\ln q_e = \ln q_D - K_D F^2 \quad (6)$$

$$E = \frac{1}{\sqrt{2K_D}} \quad (7)$$

where q_e (mg/g) is the adsorption capacity at the equilibrium time; q_D (mg/g) is the adsorption capacity;

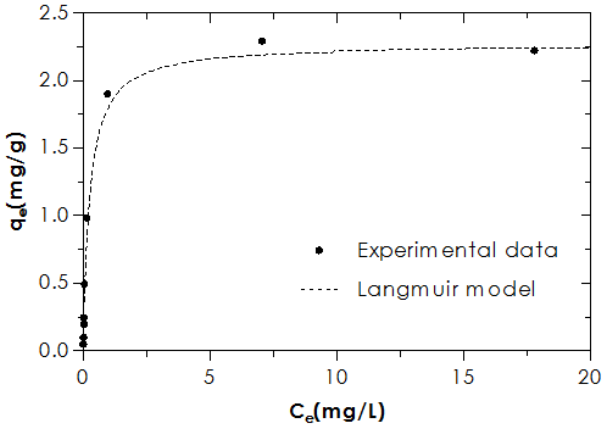

Figure 5 Adsorption isotherm of arsenate uptake onto $PC/FeCl_3$ with the experimental conditions (dosage: 10g/L, temperature: 27±1°C, pH=7±0.1, rpm=150, contact time=24h)

K_D (mol^2/kJ^2) is the activity coefficient; $F(mol^2/kJ^2) = RT\ln(1+1/C_e)$ is the Polanyi potential; R (8.31J/mol/K) is the gas constant; T (K) is the absolute temperature; and E (kJ/mol) is the mean sorption energy.

The values of q_D and K_D were obtained from the intercept and slope of the linear plot of $\ln q_e$ versus F^2 and found to be 2.21mg/g and 0.0298mol^2/kJ^2, respectively with correlation coefficient (R^2)=0.9800. The high value of R^2 implies that the D-R isotherm equation also well described the equilibrium isotherm data. The adsorption process dominates with a physical nature when 0<E<8kJ/mol, and a nature of chemical adsorption when 8kJ/mol<E<16kJ/mol [19]. The calculated value of E was 4.099kJ/mol, indicating the arsenate removal using the adsorbent was governed by a physical adsorption process.

3.5 Effect of Co-existing Anions

The arsenate adsorption efficiency of the adsorbent in the presence of various anions such as nitrate, sulfate and phosphate representing univalent, bivalent and trivalent ions, respectively, was evaluated to extend the application of the adsorbent for removing arsenate in natural water. Figure 6 shows the arsenate removal efficiency in the presence of 10 mg/L and 100 mg/L of nitrate, sulfate and phosphate applied separately and simultaneously. The degrees of

arsenate reduction from aqueous solution was NO_3^- <SO_4^{2-}<PO_4^{3-} for the separated study.

Table 3 Isotherm parameters of arsenate adsorption onto $PC/FeCl_3$

q_m(exp.) (mg/g)	Langmuir model			Freundlich model			D-R model		
	q_m(cal.)(mg/g)	K_L(L/mg)	R^2	1/n	K_F	R^2	q_D (mg/g)	E (kJ/mol)	R^2
2.22	2.27	3.8377	0.9992	0.57	1.1032	0.8703	2.21	4.099	0.9800

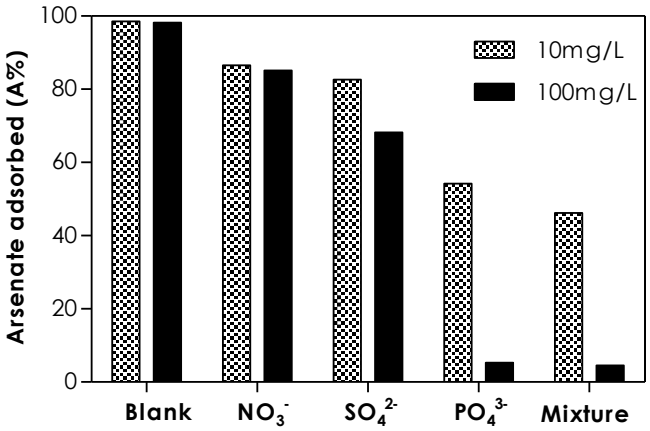

Figure 6 Effect of co-existing anions on arsenate uptake by $PC/FeCl_3$ with the experimental conditions (dosage: 10g/L, temperature: 27±1˚C, pH=7±0.1, rpm=150, contact time=24h)

The simultaneous study also showed a significant reduction compared to the blank. This implies that phosphate is possibly the main anions responsible for such great decrease of arsenate removal due to the similar structure and chemical behavior of phosphate to arsenate [20].

4.0 CONCLUSION

The broken water ceramic filter was prepared to be a mesoporous adsorbent for arsenate removal from aqueous solution. The coating method successfully increased the amount of iron oxides. The adsorption rate initially occurred fast and was slow down within 24h. The kinetic data were well described by pseudo-second order model. The high arsenate adsorption capacity of the adsorbent was resilient over pH from 4-10. The isotherm data were well fitted to the Langmuir and D-R models, providing the maximum arsenate adsorption capacity of 2.27mg/g and indicating the favorable and physical adsorption process. Among co-existing anions, phosphate showed the highest interference on the uptake capacity of arsenate. The developed mesoporous ceramic adsorbent could be considered as the effective and low cost adsorbent for arsenate removal from water due to its high uptake capacity and reutilization of local available materials considered as waste.

Acknowledgement

This study was supported by Center for Scientific and Technological Equipment (CSTE), and School of Environmental Engineering, Suranaree University of Technology, Nakhon Ratchasima 30000, Thailand.

References

[1] Chen, Y., Parvez F., Gamble M., Islam T., Ahmed A., Argos M., Graziano J. H., and Ahsan H. 2009. Arsenic Exposure At Low-To-Moderate Levels And Skin Lesions, Arsenic Metabolism, Neurological Functions, And Biomarkers For Respiratory And Cardiovascular Diseases: Review Of Recent Findings From The Health Effects Of Arsenic Longitudinal Study (HEALS) In Bangladesh. *Toxicol Appl Pharmacol*. 239(2): 184-192.

[2] Jezequel, H., and Chu K. H. 2006. Removal Of Arsenate From Aqueous Solution By Adsorption Onto Titanium Dioxide Nanoparticles. *J Environ Sci Health A Tox Hazard Subst Environ Eng*. 41(8): 1519-1528.

[3] Masih, D., Seida Y., and Izumi Y. 2009. Arsenic Removal from Dilute Solutions by High Surface Area Mesoporous Iron Oxyhydroxide. *Water, Air, & Soil Pollution: Focus*. 9(3-4): 203-211.

[4] Brammer, H., and Ravenscroft P. 2009. Arsenic in groundwater: a threat to sustainable agriculture in South and South-east Asia. *Environ Int*. 35(3): 647-654.

[5] Genc-Fuhrman, H., Bregnhoj H., and McConchie D. 2005. Arsenate Removal From Water Using Sand--Red Mud Columns. *Water Res*. 39(13): 2944-2954.

[6] Sabbatini, P., Rossi F., Thern G., Marajofsky A., and de Cortalezzi M. M. F. 2009. Iron Oxide Adsorbers For Arsenic Removal: A Low Cost Treatment For Rural Areas And Mobile Applications. *Desalination*. 248(1-3): 184-192.

[7] Mohan, D., and C. U. Jr. Pittman. 2007. Arsenic Removal From Water/Wastewater Using Adsorbents-A Critical Review. *J Hazard Mater*. 142(1-2): 1-53.

[8] Chen, R., Lei Z., Yang S., Zhang Z., Yang Y., and Sugiura N. 2012. Characterization And Modification Of Porous Ceramic Sorbent For Arsenate Removal. *Colloids and Surfaces A: Physicochemical and Engineering Aspects*. 414: 393-399.

[9] Sheng, T., Baig S. A., Hu Y., Xue X., and Xu X. 2014. Development, Characterization And Evaluation Of Iron-Coated Honeycomb Briquette Cinders For The Removal Of As(V) From Aqueous Solutions. *Arabian Journal of Chemistry*. 7(1): 27-36.

[10] Pehlivan, E., Tran T. H., Ouédraogo W. K. I., Schmidt C., Zachmann, D., and Bahadir M. 2013. Removal of As(V) from

Aqueous Solutions By Iron Coated Rice Husk. *Fuel Processing Technology*. 106: 511-517.
[11] Yadav, L. S., Mishra B. K., Kumar A., and Paul K. K. 2014. Arsenic Removal Using Bagasse Fly Ash-Iron Coated And Sponge Iron Char. *Journal of Environmental Chemical Engineering*. 2(3): 1467-1473.
[12] Kuila, U., and Prasad M. 2013. Specific Surface Area And Pore-Size Distribution In Clays And Shales. *Geophysical Prospecting*. 61(2): 341-362.
[13] Su, J., Huang H. G., Jin X. Y., Lu X. Q., and Chen Z. L. 2011. Synthesis, Characterization And Kinetic Of A Surfactant-Modified Bentonite Used To Remove As(III) And As(V) From Aqueous Solution. *J Hazard Mater*. 185(1): 63-70.
[14] Sen Gupta, S., and K. G. Bhattacharyya. 2011. Kinetics Of Adsorption Of Metal Ions On Inorganic Materials: A Review. *Adv Colloid Interface Sci*. 162(1-2): 39-58.
[15] Chang, Q., Lin W., and Ying W. C. 2010. Preparation Of Iron-Impregnated Granular Activated Carbon For Arsenic Removal From Drinking Water. *J Hazard Mater*. 184(1-3): 515-522.
[16] Fufa, F., Alemayehu E., and Lennartz B. 2014. Sorptive Removal Of Arsenate Using Termite Mound. *J Environ Manage*. 132: 188-196.
[17] Mostafa, M. G., Chen Y. H., Jean J. S., Liu C. C., and Lee Y. C. 2011. Kinetics And Mechanism Of Arsenate Removal By Nanosized Iron Oxide-Coated Perlite. *J Hazard Mater*. 187(1-3): 89-95.
[18] Khan, T. A., and Khan E. A. 2015. Removal Of Basic Dyes From Aqueous Solution By Adsorption Onto Binary Iron-Manganese Oxide Coated Kaolinite: Non-Linear Isotherm And Kinetics Modeling. *Applied Clay Science*. 107: 70-77.
[19] Ouadjenia-Marouf, F., Marouf R., Schott J., and Yahiaoui A. 2013. Removal Of Cu(II), Cd(II) And Cr(III) Ions From Aqueous Solution By Dam Silt. *Arabian Journal of Chemistry*. 6(4): 401-406.
[20] Shafiquzzam, M., Hasan M. M., and Nakajima J. 2013. Iron Mixed Ceramic Pellet for Arsenic Removal from Groundwater. *Environmental Engineering Research*. 18(3): 163-168.